Light Metals 2012 *Edited by: Carlos E. Suarez*
TMS (The Minerals, Metals & Materials Society), 2012

NUMERICAL SIMULATION ON COUPLED MULTI-FIELD OF THE PERFORATED ANODE IN ALUMINIUM REDUCTION CELLS UNDER LOW CARBON OPERATION

Hesong Li[1], Xi Cao[1], Yingfu Tian[2]
[1]School of Energy Science and Engineering, Central South University, Changsha 410083, China
[1]Chongqing Tiantai Aluminium Industry Co. Ltd, Chongqing 401328, China

Key words: the perforation structure anode, low carbon, thickness of bubble layer, coupled multi-field, numerical simulation, industrial test

Abstract

Perforation on the anode block is a new way of energy conservation. The bubbles under the anode block can be eliminated from the holes, and the energy consumption is reduced. The physical and mathematical models of perforated anode and bubble layer were established, and the thickness of the anode bubble layer and temperature field, electric field and thermal stress field were simulated. The simulation results show that the thickness of the bubble layer is 1.28cm of the perforated anode, reduced by 0.72cm compared to a normal anode, of which corresponding voltage is less than 240mV; the minimum temperature of anode block is 704.3°C, and the temperature distribution in a horizontal plane presents a wave shape due to the holes; the voltage drop of the perforated anode is 379mV and the current density distribution of the perforated anode and ordinary anode are consistent; the maximum of thermal stress is 17.4MPa in the perforated anode, which is far less than the allowable stress. The perforated anode industrial was conducted on three cells. The average cell voltage of perforated anodes decreases 229mV than the traditional reduction cell after long-term operation, which is agreed with the theoretical calculation.

Introduction

Energy efficiency is to be improved substantially in the background of low-carbon economy, and the efficiency of the most advanced aluminium technology is less than 52 percent [1,2]. About half of energy transforms into heat, which lost through the walls. Improving the equipment of the cell, reducing the energy consumption of aluminium reduction deeply, increasing the energy efficiency in the premise of unreduced the current efficiency is the development direction of the aluminium electrolysis technology in the low-carbon economy.

The high-efficiency technology of shaped cathode cells are used to weaken the wave of the liquid [3], which provides the opportunity to reduce the voltage of the aluminium reduction cell. The bubbles layer is the research object to decrease the cell voltage in the next step, and simulation and experiment methods are used together [4-7]. Slotted anode is a way to exhaust the bubbles [8-10], and used by several aluminium producers [11-14].The voltage of this anode drops by 100mV, which means the thickness of the bubbles layer reduces by 0.28cm.

The perforated structure anode is a new way to exhaust the gas below the anode to reduce cell voltage. There are several holes perforated in the anode in the vertical direction. The distance of the bubble exhausted from the bottom of the anode is less than 200mm in any bubble generation locality. The working of the bubble to overcome the electrolyte viscous force is reduced and the bubble exhausts easy and timely. The thickness of the bubble layer below the bottom of the anode and bubble infiltration distance will be decreased. The conditions for shorting polar distance, lowering working voltage and reducing electricity consumption are created.

In this paper, the physical and mathematical models of the perforated anode and the bubble layer were established, and the bubble distribution in the bottom of anode, temperature field, electric field and thermal stress field were simulated. The mechanism of the perforated anode and the influence of the holes were investigated. The industrial trials were carried out to verify the effect of the perforated anode.

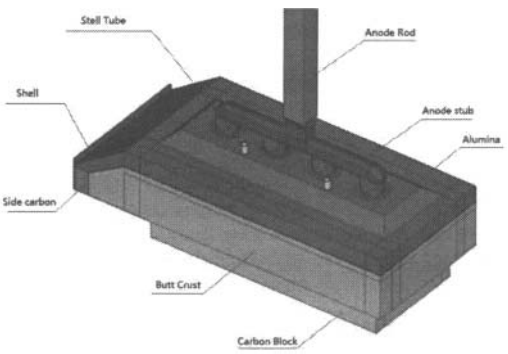

Figure 1 Perforated Anode

Perforated Anode Bubble Layer Model

The liquid aluminium and electrolyte are driven by three kinds of force in the aluminium reduction cell, which are electromagnetic force, gravity and buoyancy (caused by the temperature or the concentration gradient and by the bubbles exhausted from the anode bottom).The buoyancy factor was studied in this model, including the gas-liquid two-phase flow in the polar distance zone, and the movement of the electrolyte, which was driven by the bubbles generated in the electrochemical reaction. However the flow in the polar distance area is very complex, and there are such as electrochemical reaction, dissolution, diffusion, heat transfer and other physical processes. So this model is to make the following assumptions for such many factors:

(1) The impact of the alumina particles suspending in the electrolyte is neglected;
(2) The temperature of electrolyte and the liquid aluminium is consistent, without considering the flow caused by the temperature gradient;

(3) The bubbles do not influent the others which are generated from the neighbor anodes

CFD Model

VOF model in ANSYS-FLUENT is used to calculate the generation process and escaping process of bubbles. It is more suitable than the eulerian and mixture model for this paper to track the volume fraction of each fluid. The volume fraction equation is written as

$$\frac{1}{\rho_q}\left[\frac{\partial}{\partial t}\left(a_q\rho_q\right)+\nabla\cdot\left(a_q\rho_q\vec{v}_q\right)=S_{a_q}+\sum_{p=1}^{n}\left(\dot{m}_{pq}-\dot{m}_{qp}\right)\right] \quad (1)$$

Where m_{qp} is the mass transfer from phase q to phase p and m_{pq} is the mass transfer from phase p to phase q.

The momentum equation is

$$\frac{\partial}{\partial t}(\rho\vec{v})+\nabla\cdot(\rho\vec{v}\vec{v})=-\nabla\left[\mu\left(\nabla\vec{v}+\nabla\vec{v}^{T}\right)\right]+\rho\vec{g}+\vec{F} \quad (2)$$

The momentum equation is dependent on the volume fractions of all phases through the properties ρ and μ.

Model and Boundary Conditions

The model was established and meshed in GAMBIT, and outputted into ANSYS-FLUENT for setting the boundary conditions and solving. Only one quarter of the anode was modeled for the symmetry and simplification of calculation to simulate the gas-liquid two-phase flow of the electrolyte layer and the bubbles behavior in the bottom of the anode (Fig.2). The width of the anode is 660mm.

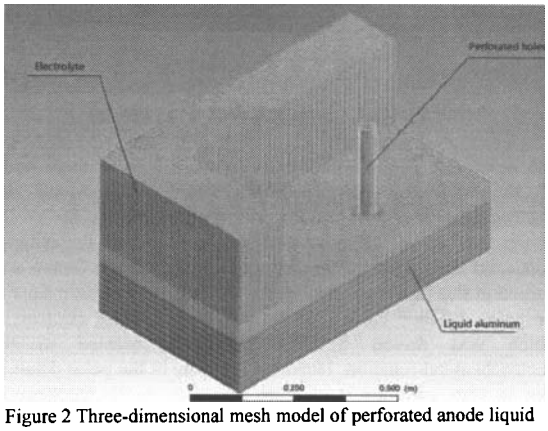

Figure 2 Three-dimensional mesh model of perforated anode liquid aluminium layer and electrolyte layer.

The problem involves large body force, such as buoyancy and gravity. Body-force-weighted scheme of pressure interpolation is suitable for this problem[15]. PISO is recommended for transient calculations for pressure-velocity coupling, while steady-state calculations will generally use SIMPLE or SIMPLEC[16]. The PISO is appropriate in this paper. The surface tension had been tested as 0.117 $N\cdot m^{-1}$ between the CO_2 and the bath. The boundary condition of the bottom of anode set as velocity-inlet. The gas velocity gets from the formula as follow:

$$V=\frac{IRT}{4FP\Phi S} \quad (3)$$

where I is current, R is the universal gas constant, F is the Faraday constant, T is the absolute temperature and P is the total pressure (Laplace + hydrostatic). Φ is gas volume fraction. S is the insert anode area.

Material Properties and Cell Process Parameters

The material properties and cell process parameters are shown in table 1.

Table 1 cell process parameters and operation parameters[17]

item	value	item	value
The current efficiency (%)	89	Bath surface tension ($N\cdot m^{-1}$)	0.177
Current(kA)	178.0	Electrolyte temperature (°C)	957
Gas density ($Kg\cdot m^{-3}$)	0.00198	Electrolyte density ($Kg\cdot m^{-3}$)	2066
Gas dynamic viscosity($Kg\cdot m^{-1}\cdot S^{-1}$)	1.49×10^{-5}	Bath dynamic viscosity ($Kg\cdot m^{-1}\cdot S^{-1}$)	2.51×10^{-3}

Results and Discussions

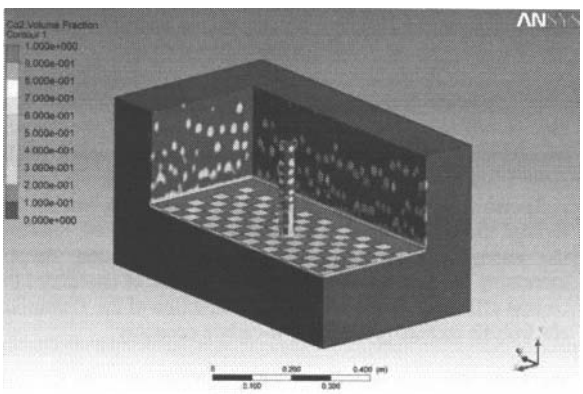

Figure 3 Two phase distribution of perforated anode bath layer gas-liquid at some moment
(Scale for CO_2 volume fraction)

Figure 3 shows the distribution of the bubbles in the electrolyte. The distribution indicates that a layer of gas filled entirely the space below the anode. The bubbles escape from the electrolyte in two methods: one is along the wall (surface of the anode), and the other one is through the holes which across the anode. Compared with the size of the holes, the thickness of the bubbles layer is about one thirds of the diameter. In fact, the thickness is 1.28cm, reduced by 0.72cm compared to a normal anode (calculated in the same method). In most instances, the current density is $0.74A/cm^2$, electrolyte resistance is 0.45Ohm/cm, and then the voltage of the polar distance reduces by

$$U_{reduce} = I \cdot R_{bath} = 0.74 \times 0.45 \times 0.72 \approx 0.24V \quad (4)$$

The calculation suggests that the cell voltage of perforated anode drops by 0.24V compared with normal cells. The result would be verified in the industrial test.

Coupled Multi-Field Model of the Perforated Anode

Due to asymmetrical distribution of temperature and asymmetrical temperature gradient, the large thermal stress emerges during the operation of aluminium cell, especially in the perforated location. If the stress grows too heavily or stress is bad-distributed seriously, the anode may be broken or shed. The stress cannot be measured for the environment in the cells, but it can be calculated using the simulation. The electric field, temperature field and thermal stress field had been calculated in the ANSYS, and the results were compared with the anode allowable stress.

The single anode physical field was studied in the assumptions as follow for the complexity:

(1) The whole of the aluminium reduction cell and its analytical domain belong to steady state;
(2) The alumina set as insulator, and the liquid set as isothermal area;
(3) The height of the bottom of anodes is consistent, and the current of each group is same, which share the whole current.

Model and Boundary Conditions

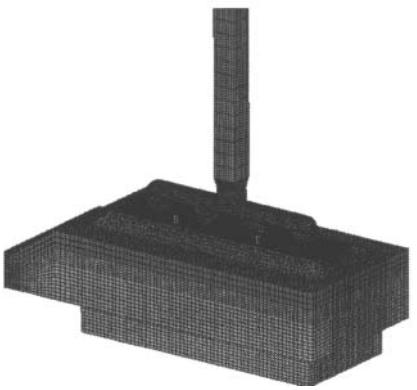

Figure 4 Perforated anode calculation mesh figure

The model includes anode, cast iron, alumina mulch, electrolyte crust, carbon sidewall and shells. The model is based on the usage of SOLID69 element together with CONTA170 and CONTA173 sharing the real constant. The coordinates defined as: X direction from the tapping end to duct end, y direction from the cell side to the middle, z direction up.

Results and Discussions

Figure 5 and 6 show that the side of the anode temperature is lower than the middle, and the most minimum temperature is located around the holes. On the surface the lowest temperature is 704.3°C, symmetrical distribution along the length direction of the anode. The temperature decreases along the holes upward inside the carbon, and the temperature of the gas exit is 338.1°C. The temperature of the bottom half of the carbon block distributes in a wave shape and the peaks is located in the perforations. The distribution indicates the temperature of bottom half of the holes is highest in the same horizontal plane due to the rising of the hot gas. The particular temperature distribution means the asymmetrical thermal stress distribution which may result the carbon broken. The thermal stress analysis is necessary.

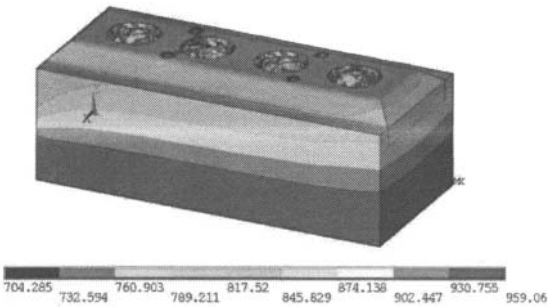

Figure 5 Temperature distribution of the carbon block (°C)

Figure 7 shows the voltage drop of the perforated carbon from the aluminium guide rod to the bottom of the carbon is 379.5mv, and the voltage drop of the carbon block is 169.5mv. The electronic field distribution is axial symmetry and no difference compared with the tradition anode.

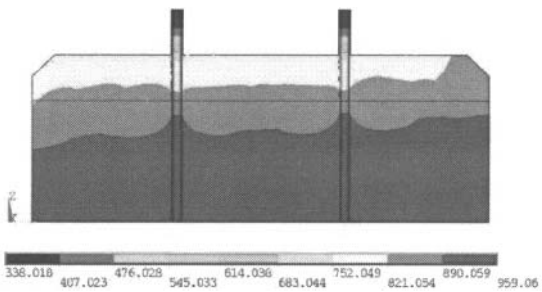

Figure 6 Temperature distribution of the perforated section (°C)

The carbon was brittle structure. According to the First and Second strength theories, the first principal stress or equivalent stress is the object to discuss. Figure 8 and 9 shows the equivalent stress distribution of the perforated anode. The thermal stress distribution agrees with the temperature distribution. The thermal stress concentrates on the contact areas of the carbon block and the cast iron and the contact areas of the carbon block and the steel tube. The maximum thermal stress is 17.4MPa, which is far less than the allowable stress of carbon. The perforated anode can be used safely as the normal carbon through the simulation calculations. However the results also need to be verified in the industrial test.

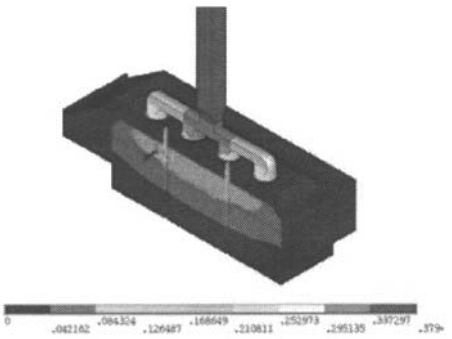

Figure 7 Electric potential of the perforated anode (V)

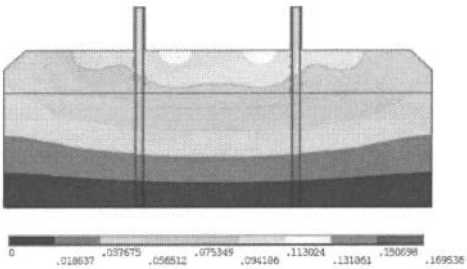

Figure 8 Electric potential distribution of the perforated section (V)

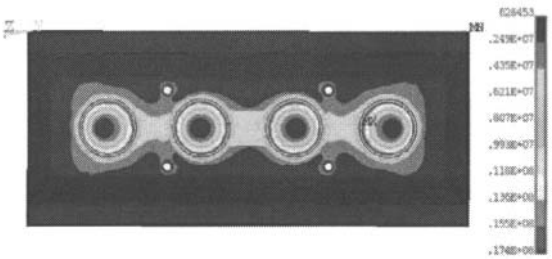

Fig.9 Thermal stress distribution of the top surface of the carbon block

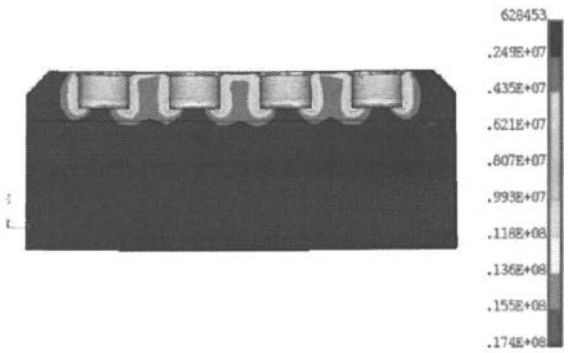

Figure 10 Perforated anode stress distribution in the center symmetry section of carbon block (MPa)

Perforated Anode Industrial Test

Perforated anodes were produced based on the improvement of the existing aluminium anode mold in Tiantai Aluminium Co. Ltd. The passing rate of Anode formed at one time vibration reached 99.2%, and shedding rate was 1.87% in work condition. The test results of perforated anode performance and that of the ordinary anode are shown in table 2.

Number 256,257 and 258 cells were selected to carry out industrial test as test cells in the 168KA aluminium reduction cells series of Tiantai. The comparison and appraisal were carried out from December 1st, 2009 to December 31st, 2010. Table 3 and 4 show the results.

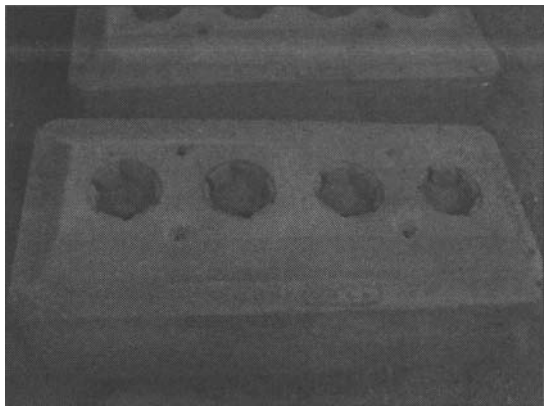

Figure 11 Perforated anodes production after baking

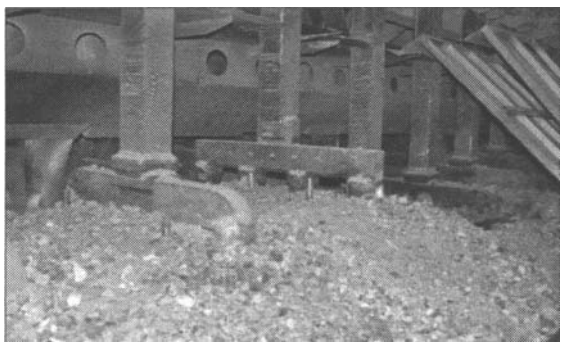

Figure 12 Perforated anodes in aluminium reduction cell

The results indicate that the average cell voltage of perforated structure dropped by 0.23V under long term industrial operation. The current efficiency increased from 91.15% to 91.85%, up by 0.7%. DC consumption reduced by 683 KWh/t-Al, and the average power consumption reached 12248 KWh/t-Al. Compared with the result, the error of the CFD simulation was 4.3%. The theoretical calculation model was correct.

Conclusion

Energy save of aluminium reduction is necessary for the low-carbon economy. But the cell voltage is not able to be decreased on the ordinary aluminium reduction cell for the steady operation. Changing the anode structure and decreasing the bubble layer is an important direction to reduce the cell voltage .

Perforated anode is a new way to decrease the bubble layer. The simulation results suggested that the thickness of the bubble layer was 1.28cm, correspondingly the cell voltage dropped by 240mv. The temperature distribution indicated the temperature of the holes was highest in the same horizontal plane. The electronic field distribution was axial symmetry and no difference compared with the tradition anode. The maximum thermal stress of the perforated anode is 17.4MPa in the operation condition, which is much less than the allowable stress.

The perforated anode was tested in three aluminium reduction cells of 168KA series in Tiantai Co.Ltd. The average voltage of test cell is 3.75V, dropped by 0.23V than the contrast cells. The net consumption of anode reduced by 23.1 Kg/t-Al, DC consumption reduced by 683 KWh/t-Al, and the average power consumption reached 12248 KWh/t-Al.

Table 2 Perforated anode physical performance assessment

Lot number	Ash content (%)	Electric resistance($\Omega mm^2/m$)	Compressive strength (MPa)	Bulk density(g/cm^3)	Actual density(g/cm^3)
17-3TK100224D22	0.47	56	43	1.6	2.06
17-3TK101207D12	0.36	55	40	1.58	2.05
17-3TK100220D18	0.37	56	39	1.57	2.05
17-3TK100215D16	0.34	54	48	1.63	2.06
National standard TY-2	≦0.8	≦60	≧30.0	≧1.50	≧2.00

Table 3 Perforated anode and ordinary anode consumption cross-references

Anode type	Average mass(Kg)	Using circle (day)	Butt height(mm)	Butt height(Kg)	Anode consumption (Kg/T-Al)	Actual consumption (Kg/T-Al)	Output in a circle(T)
Perforated anode	742	28	163	161	504.5	395.0	35.30
Contrast anode	753	29	144	121	498.7	418.1	36.24

Table 4 Technical parameters of test cell and contrast cell

Anode type	Operation voltage (V)	Metal level (cm)	Bath level (cm)	Bath temperature (°C)	Current efficiency (%)	Cryolite ratio
Perforated anode	3.75	14-16	18-20	935-345	91.85	2.5-2.6
Contrast anode	3.98	19-21	18-20	935-345	91.15	2.5-2.6

Reference

[1] C.Vanvoren, P. Homsi, J. L. Basquin. "AP 50: The Pechiney 500kA cell", Light Metals, TMS, (2007), 221-226.

[2] Xingliang Zhao, "The study of new aluminium cell heat transfer system" (M.Sc. thesis, Northeastern University, 2008), 12-13.

[3] TIAN Yingfu, "Discuss on Best Polar Distance of Industrial aluminium cell", Non-ferrous Minerals and Metallurgy, 6(25) (2009), 23-25.

[4] Kevin J. Fraser, Mark P. Taylor, and Andrew M. Jenkin. "Electrolyte Heat and Mass Transport Processes in Hall Heroult Electrolysis Cells", Light Metals, TMS, (1990), 221-226.

[5] Purdie J. M., Bilek M., and Taylor M. P., "Impact of Anode Gas Evolution on Electrolyte Flow and Mixing in Aluminium Electrowinning Cells", Light Metals, (1993) ,335-360.

[6] Xiangpeng Li, et al., "The effect on the flow field of Slotted in the bottom of the anode in the Pre-baked Aluminium reduction cells", The Chinese Journal of Nonferrous Metals, 6(16)(2006),1088-1093.

[7] Yanli Zhang, Guanghui Hou, and Shilin Qiu, "New research of the anode bubbles behavior in the aluminium reduction cell", Light Metal, 12(2007), 41-44.

[8] H.P. Diss, R. Raposo de Moura, "The use of transversal slot anodes at Albras Smelter", Light Metals, TMS, (2005), 341-344.

[9] Ketil Aldstedt Rye, "The effect of implementing slotted anodes on some key operational parameters of a PB-ling", Light Metals, TMS, (2007), 293-298

[10] Jinrong Wang, "The research and application of slotted anode in aluminium reduction cell," Minerals and Metallurgical engineering, 6(28) (2008), 251-253.

[11] Bijun Ren, Zhaowen Wang, and Zhongning Shi, "Experimental Research on Anode Grooving in Large-scale Aluminium Electrolytic Cell," Minerals and Metallurgical Engineering, 3 (27) (2007), 61-63.

[12] Binlan Xie, "Usage and manufacture of slotted anode," China Nonferrous Metallurgy, 5(2008), 79-82.
[13] Xiaoming Qin, Haisheng Sun, and Ruijun Cui, "The application of 'ship shape' anode carbon block in pre-baked anode pot", Light metal, 9(2008), 45-46.
[14] Johansen S. T., Robertson D. G. C., and Woje K., et al. "Fluid Dynamics in Bubble stirred Ladles: Part II ", Mathematical Modeling. Metallurgical Transactions B, 19B (1998), 755-764.
[15]ANSYS-FLUENT Help, "Choosing the Pressure Interpolation Scheme ",28.2.3.
[16]ANSYS-FLUENT Help, "Choosing the Pressure-Velocity Coupling Method ",28.3.1.
[17] Ping Zhou, "The Model of electromagnetic hydrodynamics in aluminium reduction cell and the simulation of the motions of melt study" (Ph.D. thesis, Central South University, 2002), 13-14.